

A novel design of dehumidifier system in underground pumped storage power station

Huimin Yao¹, Ang Li¹, Yuling Lv¹, and Xiong Shen^{1*}

¹Tianjin Key Lab of Indoor Air Environmental Quality Control, School of Environmental Science and Engineering, Tianjin University, Tianjin 300072, China

Abstract. The heavy water condensation problem has led to safety concern for the workers and electrical facilities in the underground pumped storage power station. As for current dehumidification scheme, heat and humidity load are all removed through the air conditioning unit, which has high energy consumption and low efficiency. As a large amount of moisture comes from the external fresh air, in this study, we set the dehumidification system in the underground ventilation tunnel. By using the air inlet channel to lighten the wet load, the heat and humidity parameters of the fresh air are processed as far as possible in the front of the air supply, so as to achieve the purpose of energy saving operation. In this study, numerical modelling was used to simulate the control scheme of the heat and humidity environment. Compared with the traditional method, the two new dehumidification schemes can take about 1/3 of the wet load of the main workshop, and the dehumidification efficiency is improved. Therefore, this study is expected to be a promising tool for reducing air humidity in underground workshops.

Keywords: Pumped storage power station, Underground ventilation tunnel, Dehumidification system, Heat and moisture transfer, CFD

1 Introduction

Pumped storage is an important form of energy storage, in peak regulation, accident backup and absorption of excess electric energy. Underground pumped storage power station is deeply buried underground and has the characteristics of complex cave structure, large space, multiple equipment and complex control of heat and humidity environment due to its large building volume.

The fresh air in the underground workshop of pumped-storage power station is generally introduced from the ventilation tunnel. The fresh air pretreated by the air conditioning room, and then sent to the generator layer through the air supply system when it is processed to a demanding state, so as to take the indoor heat and humidity load. According to the study of Samuelson[1] et al., the relative humidity of the air in the underground corridor is usually 80% ~ 95% in summer, and sometimes reaches 100%. High humidity not only increases the energy consumption of air conditioners, but also may lead to condensation and fogging in passageways. In addition, the humid environment leads to the discomfort of personnel and the deterioration of hygienic conditions caused by mildew, and even leads to the short-circuit failure of electrical equipment, which seriously affects the health of personnel and the safe operation of equipment.

Ventilation tunnel of underground power station is used as the main way for fresh air to enter the underground workshop. Kurnitiski[2] monitored the moisture volume and moisture exchange coefficient of underground corridor wall with natural ventilation and mechanical ventilation. The test results show that the air temperature in the underground corridor is the main factor affecting the moisture exchange coefficient, and control of moisture loss and heat action is the key factor to maintain the moisture balance. For the complex heat and humidity transfer process in large space, the numerical method has good economy and can realize the simulation of real conditions better. Therefore, numerical methods are widely used in the control of thermal and humid environment of underground powerhouse.

It can be seen that the underground corridor can pretreat fresh air to some extent. The actual effect of ventilation corridor on fresh air pretreatment under different working conditions remains to be further studied. The underground ventilation tunnel and traffic tunnel of pumped storage power station are the air inlet channels of fresh air, and the heat and moisture exchange process in the underground ventilation tunnel determines the air parameters entering the plant. If we can manage to complete the cooling and dehumidification of outdoor air in advance at the inlet side, we can reduce the load of air

* Corresponding author: shenxiong@tju.edu.cn

conditioning units.

2 Methodology

2.1 Underground plant physical model

As shown in Fig. 1., the underground plant buildings of pumped storage power station mainly include main plant, auxiliary plant, bus tunnel, main transformer tunnel, traffic tunnel, wind tunnel, etc. According to the layout of the plant, in order to reduce the total capacity of the ventilation system and increase the ventilation volume of each part, the main plant of the pumped storage power station adopts multi-level series mechanical air supply and exhaust ventilation. The ventilation tunnel is the air intake channel of underground caverns, with a total length of 1360.0m, an average slope of 5.3%, a net sectional size of 7.5m × 8.8m, and a sectional area of 55.9 m². The end of the ventilation tunnel is respectively connected with the main flexible wind tunnel and the end of the auxiliary plant.

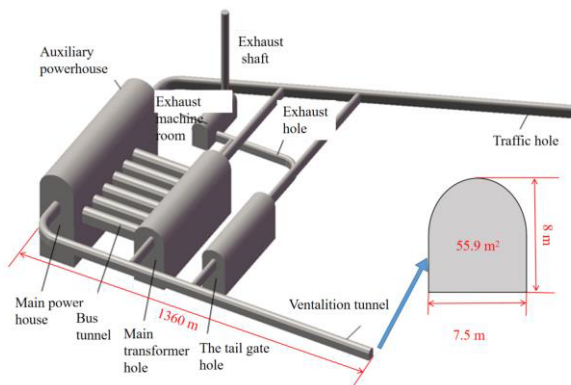


Fig. 1. Underground pumped storage power station layout

2.2 Heat and moisture transfer model

As the underground powerhouse of pumped storage power station is usually buried hundreds of meters underground, and the structure of the tunnel is complicated, the thermal and wet environment of the underground powerhouse is also affected by a variety of factors. In order to study several influencing factors, the composition of heat and humidity load of underground powerhouse is briefly analyzed.

The heat balance and wet balance equations of the envelope are selected based on lumped parameter method[3]:

$$\rho c V \frac{\partial T_0(t)}{\partial t} = Q_c(t) + Q_m(t) + Q_w(t) \quad (1)$$

$$V \frac{\partial \rho_0(t)}{\partial t} = W_c(t) + W_m(t) + W_w(t) \quad (2)$$

T_0 , Temperature, °C; V , Volume, m³; c , constant-pressure specific heat, J/(kg·°C); ρ , air density, kg/m³. In the above formula, the three on the right side of the equation are respectively the heat and humidity brought

into the room by the ventilation and air conditioning system, by equipment, personnel and lighting in the workshop and by the envelope.

2.3 Numerical model

The flow process of air in the underground workshop is mainly turbulent flow. The improved RNG K-ε two-equation model has a good effect on the simulation of large space airflow organization and heat transfer process [4]. So, RNG K-ε model is used to simulate the heat and moisture transfer process in this paper.

The gradient of physical quantity variation near the wall is very large and the wall is also a main source of turbulent vortices. In order to save computational memory and time, the wall function method is often used to arrange the first grid node in the turbulent core layer, and the connection between the viscous sub-layer and the turbulent core layer is completed by using the semi-empirical formula of the wall function. The wall function method is usually suitable for $y^+ > 15$.

According to the drawings and relevant data provided, a 1:1 geometric model of the ventilation tunnel was established. In order to facilitate the setting of boundary conditions, the ventilation tunnel was divided into 18 units along the depth direction and assigned to the corresponding boundary conditions. The wind tunnel adopts unstructured grid, the number of grids is 2.285 million, the average quality of grid is 0.86, which meets the calculation requirements of numerical simulation.

2.4 Model validation

By studying and comparing the dimensionless temperature difference and dimensionless velocity of the main workshop obtained through measurement and simulation under working conditions in summer, the accuracy test and numerical simulation results is verified. The obtained scatter diagram is shown as Fig. 2:

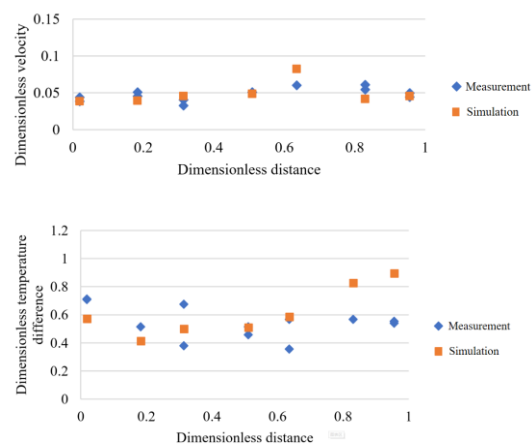


Fig. 2. Comparison between measurement and numerical simulation results of bus layer at Y=2 m

The difference between measurement and simulation is not big from the dimensionless temperature difference and velocity.

2.5 Dehumidification scheme

According to the previous analysis, combined with the design requirements and engineering practice, we put forward two schemes to arrange refrigerated dehumidifiers in the air tunnel to dehumidify outdoor fresh air as shown in fig.3. Scheme A: Set dehumidifiers in the whole section of the air tunnel, with an interval of 30 m between dehumidifiers, and arrange 90 units symmetrically on both sides of the air tunnel. Scheme B: Set dehumidifiers in the rear 1/3 section of the air tunnel, with an interval of 30 m between dehumidifiers, and arrange them symmetrically on both sides of the air tunnel. A total of 30 dehumidifiers are arranged.

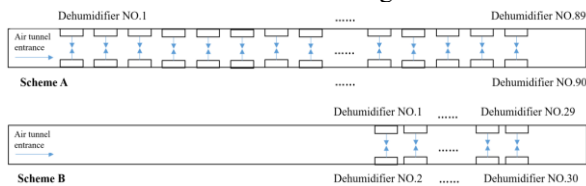


Fig. 3. Ventilation tunnel dehumidifier layout scheme

The boundary conditions of the numerical simulation are set by referring to the temperature and humidity distribution simulation of the ventilation tunnel and the related parameters of the dehumidifier. Set the air tunnel inlet and dehumidifier air supply port to velocity-inlet. The return air vent of the air tunnel and dehumidifier is set to inch-vent. Set the wall of the ventilation tunnel to wall, and the parameters are the same as those without the dehumidifier. The dehumidifier wall is set as wall, and the temperature is 27 °C.

Table 1 Boundary condition setting of numerical simulation

Site	Air tunnel entrance	Dehumidifier air supply (each)
Air supply		
Velocity m/s	3.23	2.14
Temperature °C	27.1	30
Relative humidity %	78	40
Vapor fraction	0.0182	0.0105
Blowing rate m ³ /h	650000	4000

3 Results

3.1 Heat and humidity simulation of inlet passage

Because the soil at a certain depth has great thermal inertia, the temperature of the soil in summer is lower than that of the outside air. As the outdoor air flows through the tunnel, it will be gradually cooled, and the relative humidity will increase due to the decrease of air temperature.

Fig. 4.(a) shows the temperature distribution curve of the ventilation tunnel in summer. With the increase of depth, the air temperature in the ventilation tunnel gradually decreases, from 27.1 °C at the entrance to 16.9 °C at the outlet, and the maximum temperature drop reaches

10.2 °C.

Fig. 4. (b) shows the relative humidity distribution curve of the ventilation tunnel in summer. With the increase of depth, air relative humidity increases rapidly, at about 450 m from imports, relative humidity is above 95%. Finally, the relative humidity of both outlets reached 100%. Excessive humidity in an air tunnel may cause humidity and fog in the air tunnel, which may affect personnel and equipment. Therefore, it is necessary to consider the reasonable arrangement of dehumidification equipment.

3.2 Simulation results of dehumidification scheme

3.2.1 Scheme A

Fig. 4. shows the temperature and relative humidity distribution at the outlet section. The air temperature at the outlet of the ventilation tunnel is about 18.55 °C. The temperature distribution of the outlet section of the ventilation tunnel is very uniform, and there is only a certain low temperature area near the wall. The relative humidity of the outlet section of the ventilation tunnel in scheme A is still 100%. It can be seen from the fig.4(b) that the moisture content of the tunnel through the outlet of the ventilation tunnel is 13.81 g/kg, which is 4.71 g/kg lower than that of the outdoor air. It can be seen that after the cooling of the ventilation tunnel and the refrigerated dehumidifier, the moisture content of the fresh air decreases. The air moisture content distribution at the outlet section of the ventilation tunnel gradually increases from the wall to the middle, and the air moisture content near the dehumidifier is relatively low.

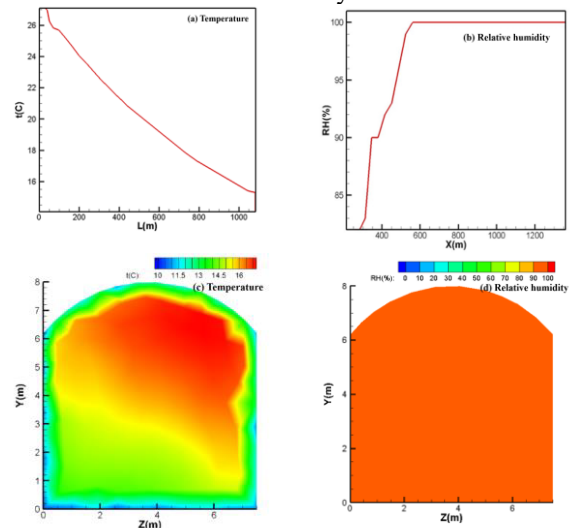


Fig. 4. The temperature and humidity variation curve and the air parameter distribution cloud diagram of the outlet section of the ventilation tunnel in summer

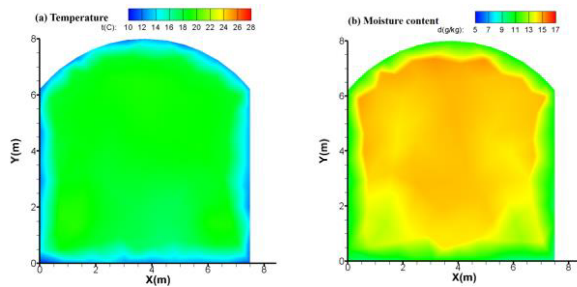


Fig. 5. Cloud diagram of temperature and humidity distribution at outlet of ventilation tunnel

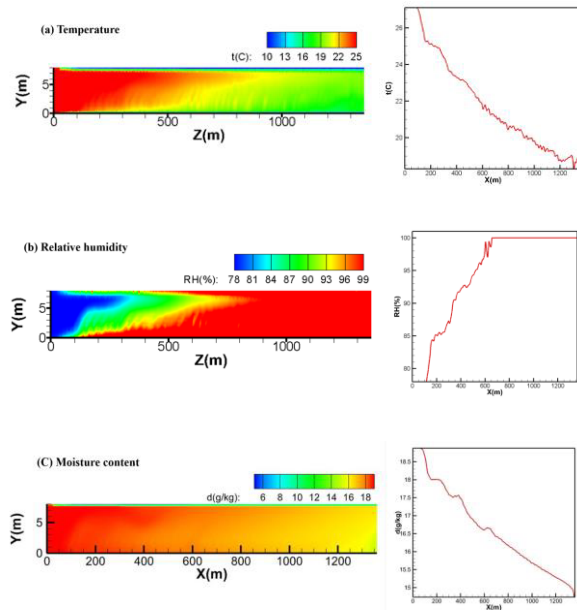


Fig. 6 The distribution cloud diagram of radial air parameters in the ventilation tunnel and the variation curve of radial air parameters in the ventilation tunnel

Fig. 6. shows the radial distribution of temperature and relative humidity in the ventilation tunnel. In order to facilitate further research on the variation rule of air parameters in the ventilation tunnel, the temperature and relative humidity distribution curves of the radial direction (Z direction) of the ventilation tunnel are drawn. With the increase of the depth, the air temperature in the ventilation tunnel gradually decreases from 27.1 °C at the entrance to 18.55 °C at the outlet. The temperature distribution in each section is not uniform.

As shown in Fig.6(b), with the increase of the depth, the relative humidity of the air in the ventilation tunnel rises gradually, from 78% to 100% at 700 m away from the entrance. The air humidity of each cross profile of the ventilation tunnel is higher in the lower areas and lower in the upper areas. Compared with the original ventilation system, the distance required for air to reach saturation in the ventilation tunnel is significantly increased. The dehumidifier made a big difference.

3.2.2 Scheme B

Fig. 7. shows the cloud diagram of air parameter distribution at the outlet of the ventilation tunnel under the arrangement mode of Scheme B. It can be seen from Fig.

7.(a) that the air temperature at the outlet of the ventilation tunnel is 17.85 °C, 9.25 °C lower than that of the outdoor air temperature. The average temperature of the outlet section of the air tunnel increases by 0.95 °C compared with that of the no dehumidifier, which is due to the higher air temperature at the air supply port of the dehumidifier heating the fresh air. The temperature distribution at the outlet section of the ventilation tunnel is very uniform, and only a certain low-temperature area exists near the wall surface. The relative humidity of the outlet section of the ventilation tunnel in this scheme is still 100%. It can be seen from Fig.7.(b) that the moisture content of the air passing through the outlet of the ventilation tunnel is 15.43g /kg, which is 3.1 g/kg lower than that of the outdoor air. It can be seen that after the cooling of the ventilation tunnel and the refrigerated dehumidifier, the moisture content of the fresh air decreases. The air moisture content distribution at the outlet cross profile gradually increases from the wall to the middle, and the moisture content near the dehumidifier is relatively low.

Fig. 8. shows the distribution of air parameters in the radial direction of the ventilation tunnel. It can be seen from the Fig.8(a) the temperature of the air in the ventilation tunnel gradually decreases from 27.1 °C at the entrance to 17.85 °C at the outlet with the increase of the depth, and the maximum temperature drop reaches 9.25 °C. The temperature distribution in cross profile of each section in the middle of the ventilation tunnel is not uniform. On the whole, the temperature in the lower areas is lower than that in the top areas, and stabilizes at about 18 °C at the first place. However, the top region gradually becomes stable after 600 m. It can be seen from Fig. 8.(b) that the relative humidity of the air in the tunnel rises gradually with the increase of the depth, from 78% to 100% of the outdoor air relative humidity. At 500 m away from the hole, the air in the ventilation tunnel reaches saturation. Compared with the situation with no dehumidifier, the distance in the ventilation tunnel for the air to reach saturation increases significantly. Compared with the simulation results of scheme A, the distance through which the air reaches saturation is shorter.

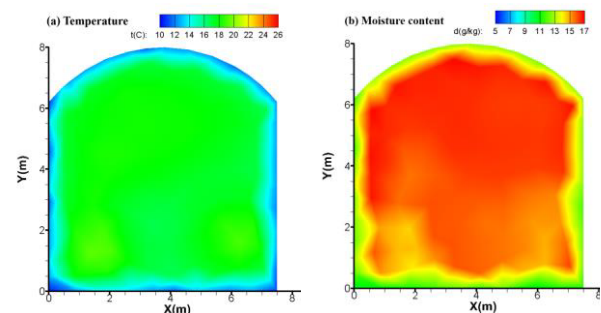
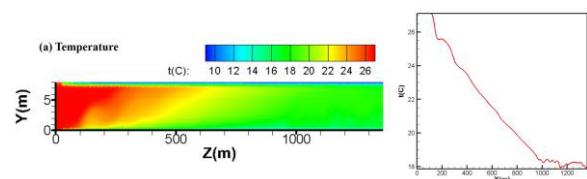


Fig. 7. Cloud diagram of temperature and humidity distribution at outlet section of ventilation tunnel



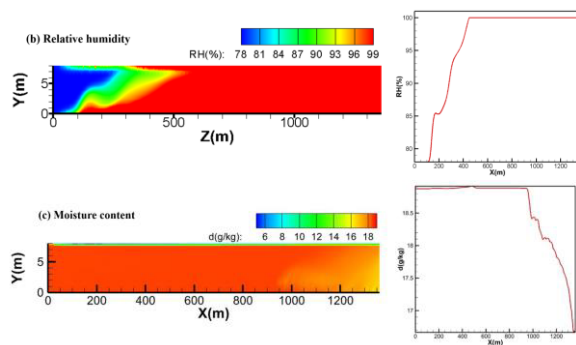


Fig. 8. The distribution cloud diagram of radial air parameters in the ventilation tunnel and the variation curve of radial air parameters in the ventilation tunnel

3.2.3 Comparison of the two schemes

After calculation, in scheme A and B, the outlet temperature of the ventilation tunnel is 18.55°C and 17.85°C, and the moisture content is 13.81g/kg and 15.43g/kg, respectively. As for scheme A, the actual wet load borne by the dehumidifier is 2258 kg/h, accounting for about 33% of the wet load of the main building. And the actual wet load of scheme B is just 1642 kg/h, accounting for about 24% of main building. Although scheme B is less effective in dehumidifying, only 30 dehumidifiers were adopted, which is more economical.

In both schemes, the relative humidity at the outlet is 100%. And the rest of the wet load needs to rely on the chiller of the main building to reduce.

4 Conclusion

In this paper, the thermal and wet environment construction method of qingyuan pumped storage power station underground powerhouse is studied.

1) Underground ventilation tunnel and the numerical model is established, and the flux of wind tunnel air temperature and humidity state parameters are analyzed in numerical simulation, the simulation results show that after the summer conditions through wind tunnel exit air temperature is 17.1 °C, relative humidity is 100%, so dehumidification process considered accordingly.

2) Then, the control schemes of the hot and humid environment are designed. The dehumidification effect of two dehumidifier layout scheme A and Scheme B are compared through numerical simulation. These two schemes can reduce the dehumidification load of the main air conditioning unit. As for dehumidifying effect, Scheme B is less effective. But it adopts only 30 dehumidifiers, which is more economical. The actual wet load of the dehumidifier under the two schemes accounts for about 1/3 of the wet load of the main building.

Reference

- [1] I. Samuelson, Moisture control in crawl space, (1994).
- [2] J. Kurnitski, Crawl space air change, heat and moisture behaviour, Energy and buildings 32(1) (2000) 19-39.

[3] C.P. Underwood, An improved lumped parameter method for building thermal modelling, Energy and Buildings 79 (2014) 191-201.

[4] A. Tsinober, An Informal Introduction to Turbulence, Fluid Mechanics and its Applications 63 (2004) 332.